

Uncertainty Quantification for Prior-Data Fitted Networks using Martingale Posteriors

Thomas Nagler, David Rügamer
 Department of Statistics, LMU Munich
 Munich Center for Machine Learning
 t.nagler@lmu.de, david.ruegamer@lmu.de

Abstract

Prior-data fitted networks (PFNs) have emerged as promising foundation models for prediction from tabular data sets, achieving state-of-the-art performance on small to moderate data sizes without tuning. While PFNs are motivated by Bayesian ideas, they do not provide any uncertainty quantification for predictive means, quantiles, or similar quantities. We propose a principled and efficient sampling procedure to construct Bayesian posteriors for such estimates based on Martingale posteriors, and prove its convergence. Several simulated and real-world data examples showcase the uncertainty quantification of our method in inference applications.

1 Introduction

Prior-data fitted networks (PFNs) are foundation models [11, 19] that allow for in-context learning, i.e., the ability to learn at inference time without any parameter updates [9]. TabPFN, a transformer pre-trained on synthetic data for in-context learning on tabular data sets, has recently attracted a lot of interest. TabPFN [11, 12] and extensions such as TuneTables [7] and LocalPFN [24] have been shown to achieve state-of-the-art performance on tabular benchmarks by pre-training on purely synthetic data. Since PFNs and extensions learn in-context, there is no need for further model (fine-)tuning on the inference task.

Recent extensions of PFNs allow their applicability to large data sets [7], the use of PFN “priors” for latent variable models [22], and simultaneously minimizing bias and variance to improve their performance [17]. PFNs are also related to simulation-based inference and amortized inference but have slightly different goals and do not amortize across a single but multiple data sets [22]. While introduced as a Bayesian method and approximation to the posterior predictive, PFNs can also be interpreted as pre-tuned untrained predictors [20]. This also relates to the question of what uncertainty PFN models can provide.

PFNs approximate the posterior predictive distribution for the label given some feature values. Despite the name, this only yields point estimates of the most relevant predictive quantities, such as the conditional mean or quantiles. Due to the complex nature of PFNs, it is difficult to assess the uncertainty of these point estimates.

We propose a principled and efficient method to construct Bayesian posteriors for such estimates using the idea of *Martingale Posteriors (MPs)*. In particular:

1. We introduce a new extension of the MP framework of [8] for inference of predictive quantities conditional on a specific feature value x .
2. We propose an efficient, nonparametric resampling scheme yielding an approximate posterior for the point estimates derived from a PFN, and prove its convergence.

3. We illustrate the new method in several simulated and real-world data applications.

Our work provides an essential tool for principled inference with the exponentially popular PFN methods. A brief discussion of potential extensions to large language models is provided in Section 5.

2 Background

We consider a tabular prediction task with labels $y \in \mathbb{R}$ and features $x \in \mathbb{R}^d$ drawn from a joint distribution P . A typical problem in such tasks is to estimate predictive quantities such as conditional means $\mathbb{E}[y|x]$, conditional probabilities $P(y|x)$, or conditional quantiles $P^{-1}(\alpha|x)$. Because the true distribution P is unknown and only a finite amount of data $\mathcal{D}_n = (y_i, x_i)_{i=1}^n$ is available, estimates of such quantities bear some uncertainty. Our goal is to quantify this uncertainty.

2.1 Prior-data fitted networks

Prior-data fitted networks are foundation models trained to approximate the posterior predictive density

$$\text{PPD}(y|x) = p(y|x, \mathcal{D}_n),$$

which quantifies the likelihood of observing label y given that the feature is x and \mathcal{D}_n has been observed. The PPD is a Bayesian concept and implicitly involves a prior over the distributions P that could have generated the data. To approximate the PPD with a PFN, a deep neural network—typically a transformer—is pre-trained on simulated data sets with diverse characteristics. After pre-training, the network weights are fixed, and the approximate PPD for a new training set can be computed through a single forward pass without additional training or tuning. The PPD quantifies uncertainty about the label y . However, it mixes the aleatoric and epistemic components of uncertainty [14]. From the PPD alone, it is impossible to disentangle these parts. Consequently, PFNs do *not* provide uncertainty estimates for predictive summaries, such as conditional mean, probabilities, and quantiles.

2.2 Bayesian inference

In classical Bayesian inference, the set of possible distributions $P = P_\theta$ is indexed by some parameter θ . A *prior* distribution $\pi(\theta)$ is elicited to quantify our beliefs about the likelihood of the possible values of θ before seeing any data. After observing \mathcal{D}_n , this belief is updated to a *posterior* $\pi(\theta|\mathcal{D}_n)$ of the parameter θ given the data. For predictive inference, the PPD can be computed as

$$\text{PPD}(y|x) = \int p_\theta(y|x) \pi(\theta|\mathcal{D}_n) d\theta.$$

In contrast to the PPD, the posterior $\pi(\theta|\mathcal{D}_n)$ also quantifies uncertainty for other interest quantities. For example, the posterior distribution for the conditional mean $\mu(x) = \int y p_\theta(y|x) dy$ is given by

$$\Pi(\mu(x) \in A) = \int \mathbb{1} \left\{ \int y p_\theta(y|x) dy \in A \right\} \pi(\theta|\mathcal{D}_n) d\theta,$$

for any $A \subseteq \mathbb{R}$. PFNs neither provide an explicit model for p_θ nor an explicit prior $\pi(\theta)$, although both may be implicit in the PPD. The following shows how Bayesian posterior inference can be approached when only the PPD is available.

2.3 Martingale posteriors

Martingale posteriors were recently introduced by [8] as a new method for Bayesian uncertainty quantification. Its core idea is to reverse the direction of the Bayesian inference. In classical Bayesian inference, the posterior is derived from a prior and likelihood, which then implicitly leads to the PPD. MP inference starts from the PPD and leaves the prior $\pi(\theta)$ implicit. An appropriate sampling scheme and Doob’s theorem then allow us to derive posteriors for virtually all quantities of interest (e.g., the conditional mean $\mu(x)$).

To simplify our outline of the approach, consider the case where there are no features, and we are interested in unconditional inference. An extension to our predictive inference setting will be made explicit in Section 3.1. Suppose we have observed data $y_{1:n} = (y_1, \dots, y_n)$.

The MP approach involves iteratively sampling

$$y_{n+1} \sim p(\cdot|y_{1:n}), \quad y_{n+2} \sim p(\cdot|y_{1:(n+1)}), \quad y_{n+3} \sim p(\cdot|y_{1:(n+2)}), \quad \dots, \quad (1)$$

N times, which yields a sample $y_{(n+1):(n+N)}$ drawn from the predictive joint distribution

$$p(y_{(n+1):(n+N)}|y_{1:n}) = \prod_{i=1}^N p(y_{n+i}|y_{1:(n+i-1)}).$$

Observe, however, that the samples are neither independent nor identically distributed. As a consequence, the long-run empirical distribution of the obtained sample,

$$F_\infty(y) = \lim_{N \rightarrow \infty} \frac{1}{N} \sum_{i=1}^N \mathbb{1}(y_{n+i} \leq y),$$

is a random function and comes out differently whenever the sampling procedure is repeated. Denote by $\Pi(F_\infty|\mathcal{D}_n)$ the distribution of this function (which depends on the data \mathcal{D}_n we start with). For any parameter $\theta = \theta(P)$ of interest, the martingale posterior is now given as

$$\Pi(\theta \in A|\mathcal{D}_n) = \int \mathbb{1}\{\theta(F_\infty)\} d\Pi(F_\infty|\mathcal{D}_n),$$

where A is any Borel set on the space where the parameter θ lives. Furthermore, Doob’s theorem [3] implies that $\Pi(\theta|\mathcal{D}_n)$ coincides with the classical Bayes posterior for the prior $\pi(\theta)$ implicit in the PPD [8].

3 Efficient martingale posteriors for prior-data fitted networks

Martingale posteriors allow for Bayesian inference directly from the PPD. PFNs approximate the PPD, so using PFNs to construct a martingale posterior seems natural. However, there are two problems. First, modern PFNs are based on transformer architectures that require $\Omega(n^2)$ operations for a forward pass on a training set size of n . Iteratively computing $p(y|y_{1:(n+k)})$ for $k = 1, \dots, N$ thus has complexity $\Omega(N^3)$, which is prohibitive. Second, [6] found that modern transformer-based LLMs substantially deviate from the *martingale property*

$$\mathbb{E}[p(y|y_{1:(n+k)})|y_{1:n}] = p(y|y_{1:n}).$$

Also TabPFN fails in this regard. Figure 1 (experiment description in Section 4.1) shows a QQ-plot of the average CDF resulting from PFN’s PPD at iteration 0 vs. the CDF after k forward iterations of the sampling procedure. The martingale property is satisfied when this distribution remains constant, i.e., all lines lie on the $x = y$ diagonal. However, we see an apparent change in the distribution over the different sampling horizons. This reinforces that PFNs approximate Bayesian inference only in a weak sense, even though they were conceived from Bayesian ideas [11, 18].

Without the martingale property, the MP sampling procedure leads to meaningless results. Instead, we propose to use the PPD implied by the PFN only as a starting point for the sampling scheme. This PPD is then iteratively updated using the nonparametric Gaussian copula approach of [8], which ensures the martingale property. The resulting martingale posterior effectively treats the PFN output as an informed prior, without requiring the PFN to provide coherent posterior updates.

3.1 Martingale posteriors for conditional inference

We extend the unconditional sampling scheme outlined in the previous section to the conditional inference setting. Fong et al. [8] already proposed one such extension. Their scheme involves forward

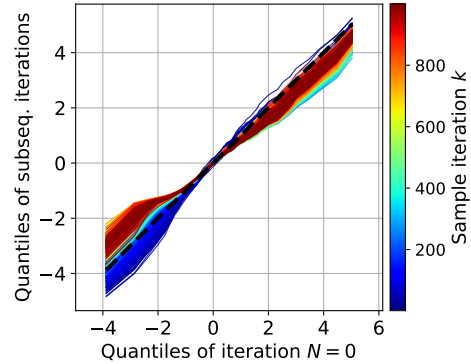


Figure 1: PFN’s initial CDF (x-axis) vs. its average CDF of subsequent iterations (y-axis).

sampling of the features $x_{(n+1):(n+N)}$. The distribution of the features isn't of primary interest but significantly complicates the sampling procedure, which the authors resolved through heuristic simplifications. In contrast to [8], we propose to sample only the labels $y_{(n+1):(n+N)}$ conditional on the event that $x_{n+k} = x$, for a fixed value of x and all $k = 1, \dots, N$.

Specifically, our goal is to simulate data from the distribution

$$p(y_{(n+1):(n+N)} | x_{(n+1):(n+N)} = x, \mathcal{D}_n).$$

Set $x_{n+k} = x$ for all $k \geq 1$, and define

$$p_k(y) = p(y_{n+k+1} | y_{1:(n+k)}, x_{1:(n+k)}),$$

and P_k as the corresponding CDF. Applying Bayes' rule recursively gives

$$p(y_{(n+1):(n+N)} | x_{(n+1):(n+N)} = x, \mathcal{D}_n) = \prod_{k=n}^{N-1} p_k(y_{k+1}),$$

which suggests that we can iteratively sample

$$y_{n+1} \sim P_0, \quad y_{n+2} \sim P_1, \quad y_{n+3} \sim P_2, \quad \dots$$

Denote the long-run empirical distribution of the obtained sample by

$$F_{\infty, x} = \lim_{N \rightarrow \infty} \frac{1}{N} \sum_{i=1}^N \mathbb{1}(y_{n+i} \leq y),$$

which is again a random function, even in the limit. Repeating the iterative sampling procedure gives us its distribution $\Pi(F_{\infty, x} | \mathcal{D}_n)$. For any conditional parameter $\theta(x) = \theta(P(\cdot | x))$ of interest, the martingale posterior is now given as

$$\Pi(\theta(x) \in A | \mathcal{D}_n) = \int \mathbb{1}\{\theta(F_{\infty, x})\} d\Pi(F_{\infty, x} | \mathcal{D}_n).$$

Common examples of the parameter $\theta(x)$ are the conditional mean

$$\theta(x) = \int y dP(y | x) dy$$

or a conditional α -quantile

$$\theta(x) = P^{-1}(\alpha | x).$$

3.2 Efficient PPD updates based on the Gaussian copula

Observe that $p_0(y) = p(y | x, \mathcal{D}_n)$ is the PPD approximated by the PFN g_θ . However, the following update distributions p_1, p_2, \dots are generally intractable. To alleviate this, [8] proposed a computationally efficient, nonparametric method based on Dirichlet Process Mixture Models (DPMMs) and a copula decomposition of the conditional p_k . Specifically, we set

$$P_k(y) = (1 - \alpha_{n+k})P_{k-1}(y) + \alpha_{n+k}H_\rho(P_{k-1}(y), P_{k-1}(y_{n+k})), \quad (2)$$

where P_k is the CDF corresponding to p_k ,

$$\alpha_i = \left(2 - \frac{1}{i}\right) \frac{1}{i+1}, \quad H_\rho(u, v) = \Phi\left(\frac{\Phi^{-1}(u) - \rho\Phi^{-1}(v)}{\sqrt{1-\rho^2}}\right),$$

and Φ is the standard normal cumulative distribution function. The method has a hyperparameter ρ , corresponding to a bandwidth that smoothes the updates. Fong et al. [8] proposed to tune this by maximizing the likelihood of the updated densities over the observed data. To increase the alignment of the updates with the PFN baseline, we simulate a new sample from the PFN and optimize the bandwidth on the simulated data.

3.3 Theoretical properties

Despite the simplicity of the updates given in Equation (2), they provide essential theoretical guarantees. The following is a direct consequence of Theorem 3 by [8].

Proposition 3.1. *It holds $(y_{N+1}, y_{N+2}, \dots) \rightarrow_d (z_1, z_2, \dots)$ as $N \rightarrow \infty$ where (z_1, z_2, \dots) has an exchangeable distribution.*

By de Finetti’s theorem (e.g., Theorem 1.49 in [23]) it then follows that there is a random variable Θ such that (z_1, z_2, \dots) is conditionally *iid* given Θ . The distribution of Θ can be interpreted as an implicit prior. In our setting, this prior depends both on the initial PPD implied by the PFN and the Gaussian copula updates specified by Equation (2). In particular, the following result follows immediately from Proposition 3.1 above and Theorem 2.2 of [2].

Proposition 3.2. *Suppose that P_0 is absolutely continuous with respect to the Lebesgue measure. Then there exists a random probability distribution $P_{\infty, x}$ such that $\lim_{N \rightarrow \infty} P_N(y) = P_{\infty, x}(y) = F_{\infty, x}(y)$ almost surely.*

The proposition implies that the (random) limit $P_{\infty, x}$ is well defined and that the iterative sampling scheme is a valid way to draw from its distribution. We can be more precise about how fast this limit is approached.

Proposition 3.3. *For any $N \geq 0$ and $\epsilon > 0$, there is a constant $C \in (0, \infty)$ such that*

$$\sup_y \limsup_{M \rightarrow \infty} \Pr(|P_M(y) - P_N(y)| \geq \epsilon) \leq 2 \exp(-\epsilon^2(n + N)/8).$$

The proof, given in Appendix A, is based on the Azuma-Hoeffding concentration inequality for martingales and relies only on the martingale property of the updates. The result quantifies how well the distribution P_N approximates $P_{\infty, x}$ after N updates. Setting $N = 0$ corresponds to the case where $P_N(y)$ equals the initial PPD given only the observed data. In our setting, this is the output from the PFN. If this PPD converges to a fixed distribution as $n \rightarrow \infty$, the proposition implies that $P_{\infty, x}(y)$ must have the same deterministic limit. Hence, the martingale posterior contracts at roughly the same speed at which the PPD converges.

Further, the approximation error decays quickly in N , so we can expect the sampling scheme to approximate $P_{\infty, x}$ well already after a moderate number of steps. Specifically, the bound implies

$$\limsup_{M \rightarrow \infty} \mathbb{E}[|P_M(y) - P_N(y)|] = O\left(\frac{1}{\sqrt{n + N}}\right).$$

The posterior of any Bayesian model contracts no faster than $1/\sqrt{n}$, even for simple, unconditional targets. Contraction rates for curve fitting problems are typically much slower [10, Chapter 9]. This suggests that a rather small number of sampling iterations suffices for negligible errors. Indeed, we observe empirically that the procedure stabilizes already after 100-200 iterations, see Figure 2.

3.4 Computation

In practice, we can only sample finite sequences and replace the MP by its finite approximation. The procedure is summarized in Algorithm 1. The overall run-time complexity of the algorithm is $O(BN)$, where B is the number of replications, and N is the length of one ‘chain’. Based on the considerations in the previous subsection, we recommend generating around $N = 200$ forward samples in each replication. The computations are independent across the outer loop iterations ($b = 1, \dots, B$) and straightforward to parallelize; the inner loop ($k = 1, \dots, N$) must be run sequentially. Except for the initial computation of $\widehat{\text{PPD}}(y | x)$, the runtime is independent of the size n of the training data set.

4 Numerical experiments

To demonstrate the efficacy of our approach, we conduct various experiments. Here, we focus on conditional posterior and coverage properties, but we also provide an unconditional posterior estimation example and comparison with classical predictive resampling in the Appendix. We use the aforementioned combination of DPMMs and copula decomposition in all cases. To estimate ρ , we always randomly draw 1000 data points simulated by the PFN.

Algorithm 1 Computation of Martingale Posterior

- 1: **Input:** Estimated $\widehat{\text{PPD}}(y|x)$ obtained from the PFN.
- 2: **for** $b = 1, \dots, B$ **do**
- 3: Initialize $P_0^{(b)} \leftarrow \widehat{\text{PPD}}(y|x)$.
- 4: **for** $k = 1, \dots, N$ **do**
- 5: Sample $y_{n+k}^{(b)} \sim P_{k-1}^{(b)}$.
- 6: Update $(P_{k-1}^{(b)}, y_{n+k}^{(b)}) \rightarrow P_k^{(b)}$ as in Equation (2).
- 7: **end for**
- 8: Compute

$$\widehat{P}_N^{(b)}(y) = \frac{1}{N} \sum_{i=1}^N \mathbf{1}\{y_{n+i}^{(b)} \leq y\}.$$

- 9: Set $\theta^{(b)}(x) \leftarrow \theta(\widehat{P}_N^{(b)})$.
- 10: **end for**
- 11: Compute the estimated Martingale Posterior:

$$\widehat{\Pi}(\theta(x) \in A | \mathcal{D}_n) = \frac{1}{B} \sum_{b=1}^B \mathbf{1}\{\theta^{(b)}(x) \in A\}.$$

4.1 TabPFN martingale property check

In order to investigate whether TabPFN possesses the martingale property, we fit TabPFN using $n = 25$ data points of a Gamma distribution with scale and shape parameter 2. Following the martingale routine in Equation (1), we then predict y_{n+k} for $k \in [1, 1000]$ and always add the previous iteration's sample to the dataset to refit TabPFN. In each step, we compute TabPFN's PPD.

Results As demonstrated in Figure 1, the resulting CDF of the iteratively updated PPD changes notably over time by first providing a wider PPD (all points of the QQ-plot lie below the bisecting line) and then becoming notably positively skewed for later iterations.

4.2 Convergence speed

We start by investigating the convergence speed analyzed in Section 3.3, in particular the results following Proposition 3.3. For this, we generate $n \in \{50, 200, 500, 2000\}$ data points from a Gamma distribution with scale parameter 1 and shape parameter 2. After standardizing the data, we visually inspect how the posterior mean distribution of y_{n+k} for $B = 30$ instances evolves when running our MP approach for $k \in (0, 200]$ steps.

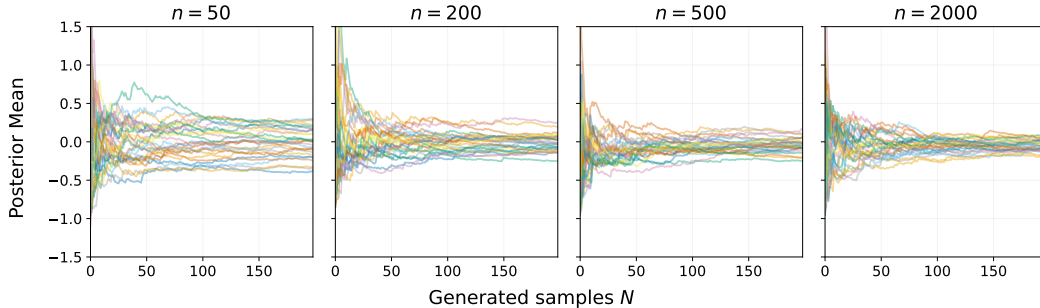


Figure 2: Effect of number of generated samples N on the convergence of P_N , depicted by $B = 30$ different PPD mean estimates.

Results Figure 2 summarizes the results and confirms that we see convergence of the different trajectories within the given budget of $N = 200$ sampling steps. While the convergence is not as fast as \sqrt{n} for smaller sample sizes, we see a positive effect of decreased variance of CDF estimates for larger values of n . This suggests that for sufficiently large n , it is not necessary to draw more than \sqrt{n} samples while $N = 200$ is sufficient for smaller n . This is confirmed in all of our practical applications where convergence is observed no later than after $N = 200$ steps.

4.3 Conditional regression posterior

As discussed in the previous section, our approach enables posterior estimation given new features x . We demonstrate this using two different regression data sets, a diffusion process ($n = 200$) and the data from [15] ($n = 400$). The diffusion process data is challenging as it evolves from an unimodal to a trimodal heteroscedastic Gaussian distribution with linear trends and sinusoidal changes depending on x . The second data set is used to evaluate how out-of-distribution (OOD) values for x affect the estimated posterior. In both cases, we use $B = 200$ replications.

Results The resulting posteriors are depicted by their respective density values in Figure 3. Both results suggest that the processes themselves and their uncertainty are well captured. For the diffusion process, it becomes apparent from the testing data that our approach can provide very accurate values for the posterior density despite the relatively few training data points. The results for the data from [16], on the other hand, confirm that our approach is also able to detect the regions of OOD values and attribute higher probability to regions further away from the PFN prediction.

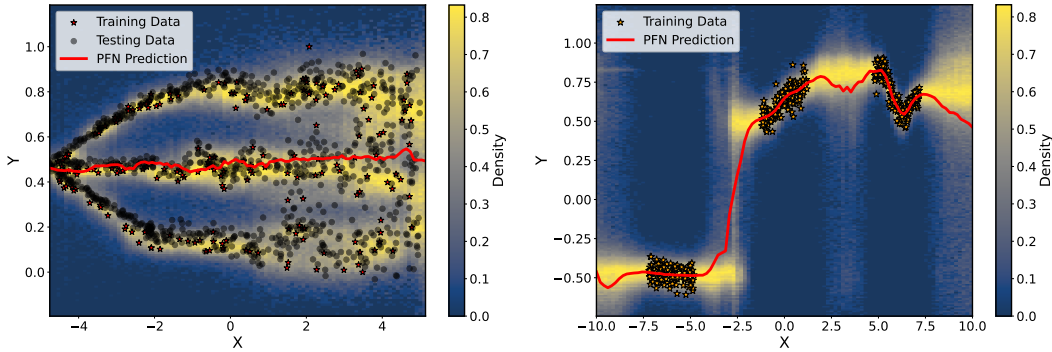


Figure 3: Visualization of PFN prediction and estimated Martingale Posterior (shaded area). Left: Diffusion process data. Right: OOD data as provided in [16].

4.4 Conditional quantile coverages

While the previous example evaluates the obtained posterior as a whole, we now investigate its coverage properties for conditional statistics. For this, we simulate data using a heteroscedastic Gaussian funnel $\mathcal{N}(\sin(3x), x^2)$ for $x \in [0, 1]$ for $n = 100$ data points. We then compute the posterior 90%-credible intervals (CIs) for the quantiles $P^{-1}(\alpha|x, \mathcal{D}_n)$, various α -levels, and three values of interest $x \in \{0.2, 0.5, 0.8\}$. For our routine, we use $B = 400$. We repeat this process 20 times with a new random data set and check how often the true quantile is included in the computed CI in each repetition.

Table 1: Coverages (\pm two std. errors) of different quantiles (columns) at different x values (rows), highlighted where ranges include the nominal coverage.

$x \backslash \alpha$	0.05	0.10	0.25	0.5	0.75	0.90	0.95
$x = 0.2$	0.65 \pm 0.21	0.60 \pm 0.22	0.65 \pm 0.21	0.75 \pm 0.19	0.80 \pm 0.18	0.85 \pm 0.16	0.85 \pm 0.16
$x = 0.5$	0.70 \pm 0.21	0.70 \pm 0.21	0.75 \pm 0.19	0.85 \pm 0.16	0.90 \pm 0.13	0.75 \pm 0.19	0.70 \pm 0.21
$x = 0.8$	0.95 \pm 0.10	0.85 \pm 0.16	0.90 \pm 0.13	1.00 \pm 0.00	0.85 \pm 0.16	0.70 \pm 0.21	0.65 \pm 0.21

Table 2: Comparison of the Martingale Posterior and Bootstrap method across datasets for conditional median regression ($\alpha = 0.5$). Reported are mean \pm standard deviation for coverage, interval length, and runtime (seconds).

	Martingale Posteriors ($B = 100$)			Bootstrap ($B = 20$)		
	Coverage	Interval Length	Time	Coverage	Interval Length	Time
airfoil	0.96 ± 0.01	0.23 ± 0.04	153.39 ± 9.31	0.91 ± 0.01	0.44 ± 0.03	328.97 ± 18.12
boston	0.93 ± 0.01	0.25 ± 0.02	67.72 ± 7.62	0.98 ± 0.02	0.51 ± 0.03	209.23 ± 13.93
concrete	0.93 ± 0.01	0.32 ± 0.05	125.38 ± 13.19	0.74 ± 0.03	0.45 ± 0.02	324.86 ± 17.52
diabetes	0.96 ± 0.03	0.70 ± 0.12	60.96 ± 14.15	0.94 ± 0.02	1.00 ± 0.06	159.72 ± 8.37
energy	0.97 ± 0.00	0.09 ± 0.02	94.70 ± 4.77	0.83 ± 0.09	0.09 ± 0.01	232.36 ± 14.36
fish	0.95 ± 0.02	0.38 ± 0.05	113.53 ± 17.79	0.94 ± 0.02	0.69 ± 0.05	212.40 ± 7.32

Results The data is visualized in Figure 6 in Appendix B. The resulting coverages are shown in Table 1. Our method provides (close to) nominal coverage for many combinations of x and α but is less accurate for $x = 0.2$ and extremal quantiles in general. This can be explained by the fact that the data at $x = 0.2$ has almost no variation, while little data is available for extreme values, making these cases very challenging given only 100 data points.

4.5 Benchmark

As a last empirical evaluation, we compare our method against a bootstrap approach on real-world data from the UCI repository [4]. The bootstrap represents the natural comparison method as it can also determine uncertainty for estimated parameters from PFN without additional assumptions. In this benchmark, we run a conditional quantile regression ($\alpha \in \{0.5, 0.9\}$) on the datasets `airfoil` ($n = 1503$, $p = 5$), `boston` ($n = 252$, $p = 15$), `concrete` ($n = 1030$, $p = 8$, [25]), `diabetes` ($n = 442$, $p = 10$, [5]), and `fish` ($n = 908$, $p = 6$). These datasets provide an ideal benchmark for PFNs, which are still limited in their scalability to larger datasets. We use 1/5th of the dataset for training and aim to measure the uncertainty of PFN for the predicted quantile on the other 4/5th of the dataset. In addition to our approach using the martingale posterior with $B = 100$, we also use a non-parametric bootstrap by rerunning the PFN method for $B = 20$ times by drawing samples from the training dataset with replacement, making quantile predictions, and compute the empirical 90% confidence interval of these predictions. We use both methods to construct a 90% credible/confidence interval (CI) and check the coverage of the predicted quantile given test dataset features. We also compute the length of these intervals to see how conservative our method is in comparison to a bootstrap approach, as well as the time for computation. We repeat the process five times with different splits.

Results Table 2 summarizes the results of our benchmark for $\alpha = 0.5$, i.e., conditional median regression. While both methods often have very close to nominal coverage or provide larger than nominal coverage, the bootstrap method fails in one case to provide a CI with close to nominal coverage. Despite having larger than nominal coverage, our MP approach consistently yields shorter or equally large CIs while often being twice as fast as the bootstrap.

In Table 3, we further show results for the quantile regression with $\alpha = 0.9$. The results are similar to those of the median regression with our approach taking a fraction of the bootstrap approach while yielding notably smaller CIs. The coverage of both methods is often close to the nominal level, while the bootstrap again struggles to estimate intervals close to nominal level for the `concrete` dataset.

5 Discussion

This work proposes an efficient and principled Bayesian uncertainty quantification method for estimates derived from prior fitted networks.

Limitations Some limitations remain in the proposed methodology. As shown below, the MP approach cannot fix severe biases in the initial PPD estimate from the PFN. Further, the current implementation does not offer credible sets that are uniform in the feature x , because there is no way to forward sample entire prediction curves. Finally, while the methodology may be applied to

Table 3: Comparison of the Martingale Posterior and Bootstrap method across datasets for conditional quantile regression ($\alpha = 0.9$). Reported are mean \pm standard deviation for coverage, interval length, and runtime (seconds).

	Martingale Posteriors ($B = 100$)			Bootstrap ($B = 20$)		
	Coverage	Interval Length	Time	Coverage	Interval Length	Time
airfoil	0.96 ± 0.01	0.25 ± 0.02	164.01 ± 11.76	0.89 ± 0.01	0.52 ± 0.03	340.42 ± 19.23
boston	0.90 ± 0.01	0.29 ± 0.02	51.48 ± 2.59	0.96 ± 0.01	0.74 ± 0.11	187.17 ± 24.83
concrete	0.88 ± 0.02	0.32 ± 0.03	145.49 ± 19.84	0.65 ± 0.05	0.56 ± 0.03	382.44 ± 80.95
diabetes	0.84 ± 0.04	0.61 ± 0.13	96.40 ± 41.68	0.92 ± 0.02	1.00 ± 0.12	238.02 ± 67.33
energy	0.96 ± 0.01	0.12 ± 0.04	101.21 ± 16.50	0.74 ± 0.06	0.14 ± 0.03	226.96 ± 17.62
fish	0.87 ± 0.03	0.45 ± 0.08	100.80 ± 8.50	0.94 ± 0.01	0.87 ± 0.13	211.07 ± 5.82

non-tabular or non-iid settings, these are currently not covered by our theory and experiments. Some potential extensions are discussed in the following.

Posteriors for other in-context learners Our theory and algorithm can be transferred directly to other in-context predictors that provide a PPD; for example, when using *large language models (LLMs)* as a prediction tool for numeric value prediction, such as in [6], or by generating so-called LLM processes [21]. Both approaches use a text-based prompt to predict future numeric values, thereby reducing the large token space to, e.g., $[0, 1]$ [6] or a 10-dimensional digit space [21].

We provide a proof-of-concept by prompting different LLMs to construct a CDF based on $n = 25$ using the setup of [6]. The prompt is given in Appendix B.4. Using the LLM output, we then run our MP approach for $N = 1000$ sampling iterations. The results are depicted in Figure 4, showing that the martingale property holds for our approach (the expected value of our generated blue CDFs coincides with the initial CDF of the LLM). While the blue curves also nicely depict the epistemic uncertainty of the LLM for the predicted CDFs, it becomes clear that the provided method—as expected—cannot counteract biases in the LLM (as is the case for GPT 4o). For more advanced LLMs, however, our approach gives uncertainty quantification akin to what is investigated [21], but potentially much cheaper.

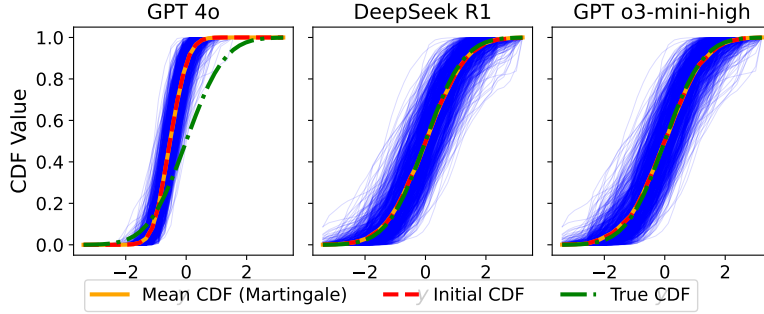


Figure 4: Predicted CDFs using different LLMs (facets) with MP uncertainty measure visualized in blue using $B = 1000$ replications and $N = 1000$ samples.

Posteriors for LLM-generated text PFNs are in-context learners based on the transformer architecture, just as modern LLMs. LLMs are trained to approximate the PPD $p(y|x, \mathcal{D})$ of the next token y given a context x of previous tokens and the corpus \mathcal{D} they were trained on. Given this similarity, the martingale posterior approach could potentially also be adapted to quantify uncertainty in LLM-generated text. There are, however, two major obstacles. First, simple PPD updates as in Equation (2) are impossible due to the complex relation between the next and the previous tokens. The complexity of such updates can likely only be matched by an equally strong LLM. Second, Proposition 3.1 and Proposition 3.2 fail due to the lack of exchangeability in the generated output tokens. Contraction results like Proposition 3.3, however, rely on only the martingale property and would remain valid, although the interpretation of the distributions P_M for $M \rightarrow \infty$ is less clear. Investigating how and to what extent martingale posterior ideas transfer to language models is an exciting path for future research.

References

- [1] Bernard Bercu, Bernard Delyon, Emmanuel Rio, Bernard Bercu, Bernard Delyon, and Emmanuel Rio. *Concentration inequalities for martingales*. Springer, 2015.
- [2] Patrizia Berti, Luca Pratelli, and Pietro Rigo. Limit theorems for a class of identically distributed random variables. *The Annals of Probability*, 32(3):2029 – 2052, 2004.
- [3] Joseph L Doob. Application of the theory of martingales. *Le calcul des probabilités et ses applications*, pages 23–27, 1949.
- [4] Dheeru Dua and Casey Graff. Uci machine learning repository, 2017. URL <http://archive.ics.uci.edu/ml>.
- [5] Bradley Efron, Trevor Hastie, Iain Johnstone, and Robert Tibshirani. Least angle regression. *The Annals of statistics*, 32(2):407–499, 2004.
- [6] Fabian Falck, Ziyu Wang, and Christopher C. Holmes. Is in-context learning in large language models bayesian? A martingale perspective. In *Proceedings of the 41st International Conference on Machine Learning*, volume 235 of *Proceedings of Machine Learning Research*, pages 12784–12805. PMLR, 21–27 Jul 2024.
- [7] Benjamin Feuer, Robin Tibor Schirrmeister, Valeriia Cherepanova, Chinmay Hegde, Frank Hutter, Micah Goldblum, Niv Cohen, and Colin White. Tunetables: Context optimization for scalable prior-data fitted networks. In *The Thirty-eighth Annual Conference on Neural Information Processing Systems*, 2024.
- [8] Edwin Fong, Chris Holmes, and Stephen G Walker. Martingale posterior distributions. *Journal of the Royal Statistical Society Series B: Statistical Methodology*, 85(5):1357–1391, 2023.
- [9] Shivam Garg, Dimitris Tsipras, Percy S Liang, and Gregory Valiant. What can transformers learn in-context? a case study of simple function classes. *Advances in Neural Information Processing Systems*, 35:30583–30598, 2022.
- [10] Subhashis Ghosal and Aad W Van der Vaart. *Fundamentals of nonparametric Bayesian inference*, volume 44. Cambridge University Press, 2017.
- [11] Noah Hollmann, Samuel Müller, Katharina Eggenberger, and Frank Hutter. TabPFN: A transformer that solves small tabular classification problems in a second. In *The Eleventh International Conference on Learning Representations*, 2023.
- [12] Noah Hollmann, Samuel Müller, Lennart Purucker, Arjun Krishnakumar, Max Körfer, Shi Bin Hoo, Robin Tibor Schirrmeister, and Frank Hutter. Accurate predictions on small data with a tabular foundation model. *Nature*, 637(8045):319–326, 2025.
- [13] David Huk, Yuanhe Zhang, Ritabrata Dutta, and Mark Steel. Quasi-bayes meets vines. *Advances in Neural Information Processing Systems*, 37:40359–40392, 2024.
- [14] Eyke Hüllermeier and Willem Waegeman. Aleatoric and epistemic uncertainty in machine learning: An introduction to concepts and methods. *Machine learning*, 110(3):457–506, 2021.
- [15] Pavel Izmailov, Wesley J Maddox, Polina Kirichenko, Timur Garipov, Dmitry Vetrov, and Andrew Gordon Wilson. Subspace inference for bayesian deep learning. In *Uncertainty in Artificial Intelligence*, pages 1169–1179. PMLR, 2020.
- [16] Pavel Izmailov, Wesley J. Maddox, Polina Kirichenko, Timur Garipov, Dmitry Vetrov, and Andrew Gordon Wilson. Subspace Inference for Bayesian Deep Learning. In *Proceedings of the Conference on Uncertainty in Artificial Intelligence*, pages 1169–1179, 2020.
- [17] Si-Yang Liu and Han-Jia Ye. TabPFN Unleashed: A Scalable and Effective Solution to Tabular Classification Problems. In *Forty-second International Conference on Machine Learning*, 2025.
- [18] Samuel Müller, Noah Hollmann, Sebastian Pineda Arango, Josif Grabocka, and Frank Hutter. Transformers can do bayesian-inference by meta-learning on prior-data. In *Fifth Workshop on Meta-Learning at the Conference on Neural Information Processing Systems*, 2021.

- [19] Samuel Müller, Noah Hollmann, Sebastian Pineda Arango, Josif Grabocka, and Frank Hutter. Transformers can do bayesian inference. In *International Conference on Learning Representations*, 2022.
- [20] Thomas Nagler. Statistical foundations of prior-data fitted networks. In *International Conference on Machine Learning*, pages 25660–25676. PMLR, 2023.
- [21] James Requeima, John F Bronskill, Dami Choi, Richard E. Turner, and David Duvenaud. LLM processes: Numerical predictive distributions conditioned on natural language. In *The Thirty-eighth Annual Conference on Neural Information Processing Systems*, 2024.
- [22] Arik Reuter, Tim G. J. Rudner, Vincent Fortuin, and David Rügamer. Can transformers learn full bayesian inference in context? In *Forty-second International Conference on Machine Learning*, 2025.
- [23] Mark J Schervish. *Theory of statistics*. Springer Science & Business Media, 2012.
- [24] Valentin Thomas, Junwei Ma, Rasa Hosseinzadeh, Keyvan Golestan, Guangwei Yu, Maks Volkovs, and Anthony L Caterini. Retrieval & fine-tuning for in-context tabular models. *Advances in Neural Information Processing Systems*, 37:108439–108467, 2024.
- [25] I-C Yeh. Modeling of Strength of High-Performance Concrete Using Artificial Neural Networks. *Cement and Concrete research*, 28(12), 1998.

A Proof of Proposition 3.3

We use arguments similar to [8]. It holds

$$\mathbb{E}[P_M(y)|y_{(n+1):(n+M-1)}] = (1 - \alpha_{n+M})P_M(y) + \alpha_{n+M}\mathbb{E}_{y_{n+M} \sim P_{M-1}}[H_\rho(P_{M-1}(y), P_{M-1}(y_{n+M}))].$$

By the probability integral transform, it holds $P_M(y_{n+M+1}) \sim \text{Uniform}[0, 1]$. Thus,

$$\mathbb{E}_{y_{n+M} \sim P_{M-1}}[H_\rho(P_{M-1}(y), P_M(y_{n+M}))] = \int H_\rho(P_{M-1}(y), u)du = P_{M-1}(y),$$

by the properties of the Gaussian copula. Hence,

$$\mathbb{E}[P_M(y)|y_{(n+1):(n+M-1)}] = P_{M-1}(y),$$

which implies that $P_M(y)$ is a martingale. Furthermore,

$$|P_M(y) - P_{M-1}(y)| \leq \alpha_{n+M} \leq \frac{2}{n + M + 1}, \quad \text{for all } y \in \mathbb{R},$$

and

$$\sum_{i=N}^{\infty} \alpha_{n+i}^2 \leq \int_N^{\infty} \frac{4}{(n+t)^2} dt \leq \frac{4}{n+N}.$$

Now the Azuma-Hoeffding inequality (e.g. [1]) yields

$$\Pr(|P_M(y) - P_N(y)| \geq \epsilon) \leq 2 \exp\left(-\frac{\epsilon^2}{2 \sum_{i=N}^{\infty} \alpha_{n+i}^2}\right) \leq 2 \exp\left(-\frac{\epsilon^2(n+N)}{8}\right).$$

□

B Further numerical experiments and details

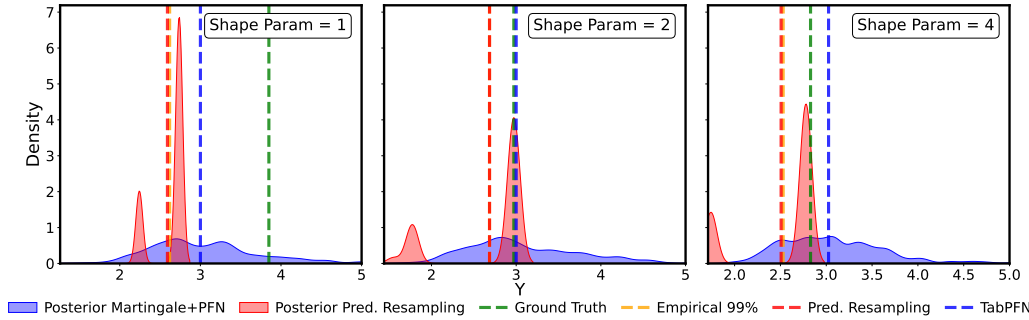


Figure 5: Comparison of the posterior from our method (blue) and the one obtained by predictive resampling (red) for different shape parameters γ (columns) of the Gamma distribution.

B.1 Unconditional quantile posterior

We here provide another experiment where we analyze the ability of our approach to estimate the posterior of an extreme quantile of a skewed distribution. For this, we simulate a Gamma distribution with different shape parameters $\gamma \in \{1, 2, 4\}$, inducing varying left-skewness. We then task PFN to estimate the 99%-quantile (the function T) and use our approach to compute the posterior uncertainty for PFN's estimate. In this experiment, we use $B = 1,000$ replications and $N = 10,000$. To make the task of quantile estimation more challenging, we use a relatively small data set size of $n = 25$. To evaluate the performance, we compare the distribution against the true value and a posterior estimate by the predictive resampling approach from [8] that does not have access to the PFN.

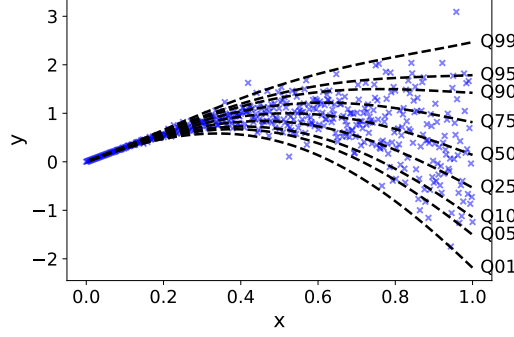


Figure 6: Depiction of the data used in Section 4.4.

Results An exemplary result for the posteriors for different shape values is visualized in Figure 5, showing the general trend of the results. The predictive resampling methods, which do not have access to the simulated data from TabPFN, usually result in a much more concentrated and bimodal posterior. This, however, comes at the cost of not always covering the true value. In contrast, the posterior for our method is much wider, thereby always covering the true value independent of the shape parameter.

B.2 Data generation for diffusion process

For the diffusion process data in Section 4.3, we use the following data-generating process:

1. Input generation: The input variable x is sampled uniformly from $[2.5, 12.5]$.
2. Piecewise functional behavior: The output y is determined by three different functions applied to x , separated by a data-dependent midpoint m , approximately at $\text{median}(x) - 2$. The three functional forms are:
 - $f_1(x)$: A linear and sinusoidal function switching at m .
 - $f_2(x)$: A mirrored version of $f_1(x)$.
 - $f_3(x)$: A piecewise function with a constant component and a high-frequency sine term.

Each sample is randomly assigned one of these three functions.

3. Heteroscedastic noise: Additive noise is introduced with a scale that increases quadratically with x , making uncertainty larger for larger x .
4. Output transformation: The input is centered to be within $[-2.5, 2.5]$, and the output values are normalized based on their min-max range for potential use in quantile-based learning.

B.3 Data generation for quantile regression

For the data in Section 4.4, we sample values $x \sim U(0, 1)$ and generate the corresponding outcome via $y \sim \mathcal{N}(\sin(3x), x^2)$. A visualization of the data set is given in Figure 6.

B.4 Prompt for LLMs

The prompt used for the experiment in our discussion is given as follows:

```
Given the following data which are i.i.d. sampled from a Gaussian,
-1.609 -0.384 -0.592 0.073 -1.998 -1.093 -1.033 -3.159 -1.714 -2.754 0.832
1.294 0.411 -1.168 -1.246 -1.279 -1.488 0.376 -1.554 -0.318 1.267 0.836
-1.456 -1.921 -2.545
generate the CDF of the posterior predictive for a new value,
evaluated at the following data points:
-5 -4.75 -4.5 -4.25 -4 -3.75 -3.5 -3.25 -3 -2.75 -2.5 -2.25 -2 -1.75 -1.5
-1.25 -1 -0.75 -0.5 -0.25 0 0.25 0.5 0.75 1 1.25 1.5 1.75 2 2.25 2.5 2.75 3
```

B.5 Computational environment

All computations were performed on a user PC with Intel(R) Core(TM) i7-8665U CPU @ 1.90GHz, 8 cores, 16 GB RAM using Python 3.8, R 4.2.1, and TensorFlow 2.10.0. Run times of each experiment do not exceed 24 hours.

All experiments that use TabPFN are done with `tabpfn==2.0.5`. GPT 4o and GPT o3-mini-high are called via OpenAI’s UI. DeepSeek R1 is called from its UI at www.deepseek.com. All other methods are implemented from scratch by the authors.

C Further discussion

Another open problem is joint posterior inference for a collection of parameters $\theta = \{\theta(x) : x \in \mathcal{X}\}$. Although our proposed inference procedure can be repeated for many values of x , the resulting posteriors are disconnected. For obtaining a full joint posterior $\Pi(\theta|\mathcal{D}_n)$, the distribution of the features $x_{1:n}$ can no longer be ignored. [8] proposed a general joint update of the PPDs for all values of x simultaneously. However, this general update is intractable, and the heuristic simplifications proposed by [8] are neither particularly simple nor theoretically justified. There are several potential ways forward. A simple practical solution would be to specify a joint distribution that combines the individual posteriors $P_{\infty, x_1}, \dots, P_{\infty, x_K}$ in a plausible way; for example, using a multivariate Gaussian copula with covariance kernel depending on the distance between values $x_i \neq x_j$. We expect such a heuristic correction to work reasonably well in many applications. A more sophisticated alternative was recently proposed by [13] and involves nonparametric estimation of the implicit dependence between PPDs by a nonparametric vine copula.